



HAL
open science

Original Synthesis of Molybdenum Nitrides Using Metal Cluster Compounds as Precursors: Applications in Heterogeneous Catalysis

Kevin Guy, Franck Tessier, Helena Kaper, Fabien Grasset, Noee Dumait, Valérie Demange, Mitsuaki Nishio, Yoshitaka Matsushita, Yoshio Matsui, Toshiaki Takei, et al.

► To cite this version:

Kevin Guy, Franck Tessier, Helena Kaper, Fabien Grasset, Noee Dumait, et al.. Original Synthesis of Molybdenum Nitrides Using Metal Cluster Compounds as Precursors: Applications in Heterogeneous Catalysis. *Chemistry of Materials*, 2020, 32 (14), pp.6026-6034. 10.1021/acs.chemmater.0c01369 . hal-02928629

HAL Id: hal-02928629

<https://hal.science/hal-02928629>

Submitted on 3 Sep 2020

HAL is a multi-disciplinary open access archive for the deposit and dissemination of scientific research documents, whether they are published or not. The documents may come from teaching and research institutions in France or abroad, or from public or private research centers.

L'archive ouverte pluridisciplinaire **HAL**, est destinée au dépôt et à la diffusion de documents scientifiques de niveau recherche, publiés ou non, émanant des établissements d'enseignement et de recherche français ou étrangers, des laboratoires publics ou privés.

Original Synthesis of Molybdenum Nitrides Using Metal Cluster Compounds as Precursors: Applications in Heterogeneous Catalysis

Kevin Guy^{1,2,3}, Franck Tessier¹, Helena Kaper³, Fabien Grasset^{2,4}, Noée Dumait¹, Valérie Demange¹, Mitsuaki Nishio⁴, Yoshitaka Matsushita⁴, Yoshio Matsui⁴, Toshiaki Takei⁵, David Lechevalier^{2,4}, Caroline Tardivat³, Tetsuo Uchikoshi^{2,4}, Naoki Ohashi^{2,4}, Stéphane Cordier¹

¹Univ. Rennes – CNRS – Institut des Sciences Chimiques de Rennes, UMR 6226, 35000 Rennes, France

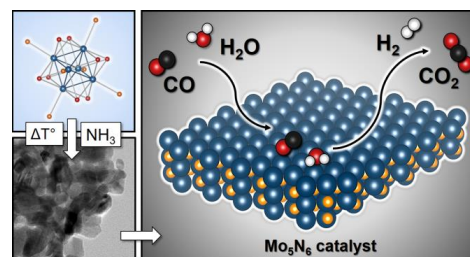
²CNRS – Saint-Gobain – NIMS, UMI 3629, Laboratory for Innovative Key Materials and Structures (LINK), National Institute for Materials Science, 1-1 Namiki, 305-0044 Tsukuba, Japan

³CNRS – Saint-Gobain Research Provence, UMR 3080, Ceramic Synthesis and Functionalization Laboratory, 84306 Cavaillon, France

⁴Research Center for Functional Materials, National Institute for Materials Science, 305-0044Tsukuba, Japan

⁵Research Center for Materials Nanoarchitectonic, National Institute for Materials Science, 305-0044Tsukuba, Japan

ABSTRACT: Transition metal nitrides (TMN) form a class of materials with unique physical and chemical properties. Among them, molybdenum nitrides are mainly used as high-performance magnets or catalysts for a wide range of reactions. This work aims at developing innovative syntheses to prepare nanostructured TMN from metallic clusters for heterogeneous catalysis. The use of a nanoscale precursor such as $(\text{TBA})_2\text{Mo}_6\text{Br}_{14}$ (TBA = tetrabutylammonium = $(\text{C}_4\text{H}_9)_4\text{N}^+$) enables to reach different molybdenum nitride compositions (Mo_2N , Mo_5N_6) by thermal reaction under ammonia at relatively low temperatures. Such a novel synthetic approach highlights the prime importance of the starting material to stabilize specific stoichiometries. The impact of this new synthetic route is characterized by several techniques including electron probe microanalysis and high-resolution transmission microscopy. Moreover, catalytic properties of these potential cost-effective catalysts are investigated for the Water-Gas Shift Reaction.



• INTRODUCTION

The main objective of this work is to develop an innovative synthetic route leading to molybdenum nitrides using nanostructured precursors, i.e. octahedral molybdenum halides-based cluster compounds¹. From a panel of compositions, we focus the study on the thermal reaction of the $(\text{TBA})_2\text{Mo}_6\text{Br}_{14}$ cluster under flowing ammonia. Depending on the temperature, this cluster favors the formation of single-phase Mo_2N and Mo_5N_6 nitrides. We aim to use such a nanoscale precursor to form nanostructured nitrides at low temperatures in comparison with common synthetic routes^{2,4}, leading to higher specific surface areas, and enhanced catalytic activities. Our first results as detailed below demonstrate the efficiency of the solid-gas reaction between a Mo_6 cluster and ammonia as an efficient route to produce molybdenum nitrides. Specific attention is paid on the physicochemical characterizations of the different intermediates from the precursor level (cluster) to the final nitride, with a particular focus on the ageing of samples. Molybdenum nitrides, as well as other transition metal nitrides (TMN), can be considered as nitrogen insertion compounds in the metal network. The metal generally forms a face-centered cubic (fcc) or hexagonal (hex.) closed-packed network in which the nitrogen atoms occupy the trigonal prismatic or octahedral sites. Besides well-known stoichiometric MoN (hex.) and Mo_2N

(fcc), an original bulk Mo_5N_6 (hex.) single phase was obtained to date only by nitriding a MoS_2 precursor with a high specific surface area at 700°C ^{4,5}. The structure can be described as a stacking of prisms and octahedra of nitrogen, where nitrogen atoms are of the AABB type (like sulfur in MoS_2). The octahedral sites have a 66% occupancy level whereas molybdenum atoms occupy all the prismatic sites. Vajenine et al.² confirmed the space group $P6_3/m$ by studying a mixture of Mo_5N_6 and $\delta\text{-MoN}$ phases. However, in contrast to Tessier et al.⁵, their structural model implies to place the vacancies on the prismatic sites and not on the octahedral sites. Recently, Khalifah et al.⁶ concluded that the molybdenum vacancies are placed on the octahedral sites and tried to assign Mo_5N_6 in the $P6_3/mcm$ space group, with a model really close to the one defined by Tessier et al. (Figure S1 and Table S1).

TMN have properties close to metals (optical, magnetic and electrical properties) and ceramics (high hardness and melting points), making these compounds a particular class of materials. Interstitial nitrides are often compared to platinoids (platinum, gold) due to their convincing catalytic properties without exceeding their performances, but for much lower costs⁷⁻⁹. In recent years, several groups have studied the synthesis of new cost-efficient catalysts in finding alternatives to these expensive noble metals listed as critical raw materials¹⁰.

As an illustration, Mo₂N was tested for the hydrogen evolution reaction¹¹⁻¹⁴ and for hydro-denitrogenation^{15,16}, Mo₂N and Co₃Mo₃N for ammonia synthesis¹⁷⁻¹⁹, Mo₂N for hydrazine decomposition²⁰, VN and Mo₂N for ethanol amination reaction²¹, Mo₂N and W₂N for base catalysis^{22,23}. Concerning Mo₅N₆, only few examples of applications are listed in the literature. Recently, Mo₅N₆ has been tested for applications in electrocatalysis^{6,31}. All these nitrides often stand out for their catalytic activities in comparison with those of the catalysts usually tested⁷. Mo₂N and Mo₅N₆ are tested in this work as heterogeneous catalysts, in particular for the water-gas shift reaction (WGSR): CO + H₂O → CO₂ + H₂. The WGSR takes place in several industrial processes: ammonia synthesis, methanol synthesis or Fischer-Tropsch process. Recently, it was used in proton exchange membrane fuel cells in order to transform carbon monoxide, toxic for the cell membrane, into non-toxic CO₂²⁴. In addition, it allows the production of hydrogen (H₂) from water vapor, useful for the operation of the fuel cell. With the search for alternatives to combustion engines, a renewed interest in the synthesis of effective catalysts for the WGSR appeared, using for example Au supported on molybdenum carbides²⁵ or metal-oxide supported platinum and gold²⁶⁻³⁰. Here, we show for the first time the performance of Mo₅N₆ for the WGSR.

• EXPERIMENTAL SECTION

Synthesis Precursors synthesis (TBA)₂Mo₆Br₁₄ (TBA = TetraButylAmmonium: (C₄H₉)₄N⁺) is obtained by cationic metathesis by addition of (TBA)Br in a solution of Cs₂Mo₆Br₁₄ dissolved in a water/ethanol mixture¹. Cs₂Mo₆Br₁₄ is prepared from stoichiometric amounts of MoBr₂ and CsBr in a vacuum-sealed silica tube heated at 950°C for three days. (TBA)₂Mo₆Br₁₄ (TMB) crystallizes in the P₂₁/n space group. Stacking of [Mo₆Br₁₄]²⁻ cluster units corresponds to a distorted centered cubic arrangement. TMB (JCPDS file 98-810-1712) cluster compound is synthesized with a specific surface area of 1 m²/g, and 4.5 wt.% (O) due to the use of H₂O and EtOH as solvents.

MoS₂ (JCPDS file 00-024-0513) is prepared at 350°C in KSCN melt starting from commercial MoO₃ (Acros Organics CAS 1313-27-5 ; 1 m²/g)³². As-prepared MoS₂ has a specific surface area of 200 m²/g and contains 3.5 wt.% (O) due to the large specific surface area combined with ambient conditions.

Nitrides synthesis TMB, as-prepared MoS₂ and commercial MoO₃ are pretreated at 150°C under vacuum conditions to clean their surfaces. Then, precursors are placed in an alumina boat and heated under flowing ammonia at a flow rate of 30 L/h in the temperature range of 400-700°C, with a heating rate of 5°C/min. After a dwelling time of 16-48 hours, the furnace was switched off and the nitride product was cooled down to room temperature in a pure nitrogen atmosphere.

Characterization X-Ray diffraction (XRD) Patterns were recorded in the 10-90° 2θ range on a Panalytical X'PERT Powder (Cu Kα, 40 kV, 40 mA) diffractometer equipped with a PIXcel 1D detector. All phase analyses were

performed using the HighScore Plus software. Rietveld refinement were conducted using the FullProf Suite software.

Elemental analyses Nitrogen and oxygen contents were determined with a LECO® TC-600 analyzer using the inert gas fusion method. Nitrogen was measured as N₂ by thermal conductivity and oxygen as CO₂ by infrared detection. The apparatus was calibrated using LECO® standards. Although water contamination, adsorbed species or high specific surface area powders are examples of situations that can affect seriously the analyses, the hot extraction technique appeared to be one of the most efficient method to get rapid and reliable O and N contents³³.

Specific surface area The Brunauer-Emmet-Teller (BET) specific surface area was determined from nitrogen physisorption with a Micromeritics Gemini VII 2390t instrument using a mixture of N₂/He (30%/70%). To avoid the surface hydration, samples were previously outgassed under vacuum at 100°C.

Transmission electron microscopy (TEM) TEM and high resolution TEM (HRTEM) images were acquired on a JEM-2100F (JEOL Co.) at 200 kV. Compositional analyses were performed by Energy Dispersive X-ray Spectroscopy (EDS) with double wide detecting area (100 mm²) detectors equipped in a JEM-2800 (JEOL Co.) operating at 100 kV. A small amount of molybdenum nitrides was dispersed in ethanol, placed on a net like carbon film covered Cu grid (Cu micro grid), and dried in ambient conditions.

Electron probe microanalyses (WDS-EPMA) The mapping analyses on molybdenum nitrides were recorded by electron probe microanalysis (EPMA) on a wavelength dispersion spectrometer (WDS) (JEOL JXA-8900R equipment). WDS mapping measurements were conducted at an acceleration voltage of 15 kV on a 500 x 500 μm range.

Thermogravimetric analyses (TGA-MS) The TGA were recorded on a temperature range between 30 and 550°C with a ramp of 5°C/min using a LabSysEvo TGA by Setaram, coupled with a Pfeiffer Omnistar GSD 320 mass spectrometer to record the following m/z signals: 12, 14, 15, 16, 17, 18, 28, 30, 32 and 44.

Table 1: Ammonolyses realized on several molybdenum-halides cluster compounds, synthesis conditions & products obtained.

Precursor	Ammonolysis T (°C)	Product(s)
Cs ₂ Mo ₆ Br ₁₄	400	Mo ₂ N + CsBr
	500	MoN + CsBr
Cs ₂ Mo ₆ Cl ₁₄	400	Mo ₂ N + CsCl
	600	MoN + CsCl
(NH ₄) ₂ Mo ₆ Br ₁₄	400	Mo ₆ Br ₁₂
	500	MoN + Mo ₂ N
(TBA) ₂ Mo ₆ Br ₁₄	450	Mo ₂ N
	500	Mo ₅ N ₆

Catalytic tests (WGSR) The catalytic performances of the molybdenum nitrides for the WGSR were studied in the temperature range between 150 and 550°C with a heating rate of 2°C/min. The feed gas was composed of 5 mol.% CO, 25 mol.% H₂O and He as a carrier gas, with a constant flow rate of 80 mL/min. Water vapor was introduced at 30°C with a flow of 0.12 g/h, using a Bronckhorst CEM flowmeter. An online μ GC coupled with a TCD and equipped with two columns (MolSieve5APLOT and Column PLOT U), was used to measure the concentrations of CO and CO₂. All catalysts were sieved between 150 and 250 μ m, weighted (0.1 g) and diluted in SiC (0.3 g) to obtain a homogeneous catalytic bed. Stability tests were realized after three successive light-off on each sample. The thermal equilibrium presented on Figure 7 and Figure 8 is extracted from the work of Chein et al.³⁴. Carbon balance is calculated using the following formula: CO consumed minus CO₂ formed, divided by initial CO concentration.

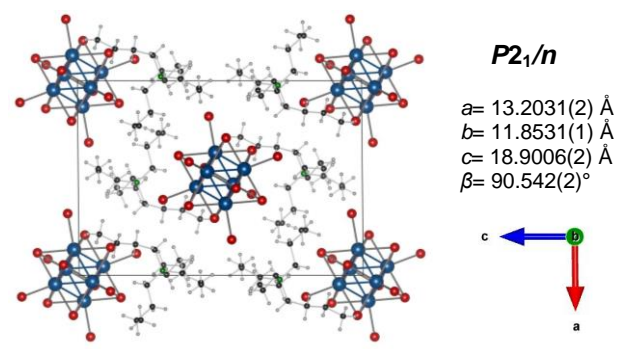


Figure 1. Projection of the TMB unit cell along the [010] direction and lattice parameters¹

• RESULTS AND DISCUSSION

Choice of the precursor As defined by Cotton et al.³⁵ cluster compounds are aggregates of finite dimensions of metal atoms connected to each other by metal-metal bonding. Transition metal cluster compounds are widely used for their luminescence or UV-NIR absorption properties³⁶⁻⁴⁰. In this work, the true nanoscale aspect (\approx 1 nm) of these compounds is used in order to form nanostructured molybdenum nitrides. Several molybdenum cluster compounds are treated at different temperatures under a fixed ammonia flow of 30L/h. The starting compounds reported in **Table 1** are those that

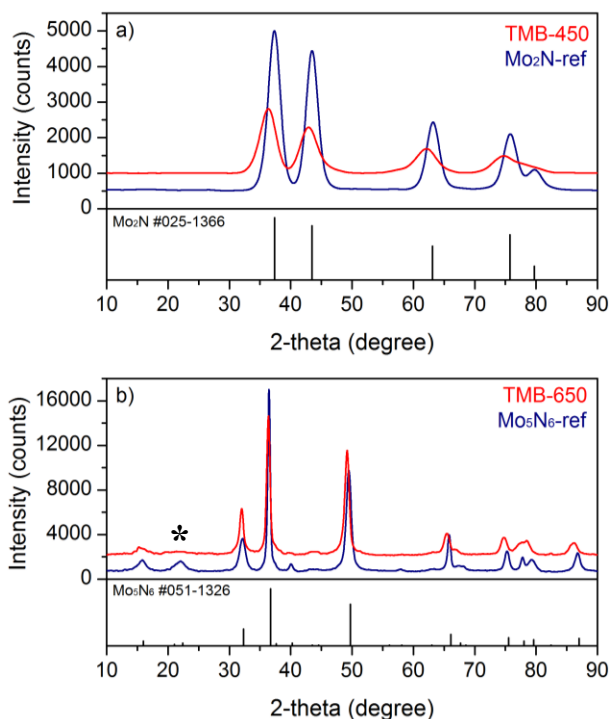


Figure 2. Powder-XRD patterns of Mo₂N samples: TMB-450 and Mo₂N-ref (a) and Mo₅N₆ samples: TMB-650 and Mo₅N₆-ref (b).

give the best results among a wider A₂Mo₆X₈X₆^a series differing by the nature of A⁺ counter cations and X halides. Precursors containing cesium counter-cations lead to the formation of CsBr/CsCl in the final material due to the thermal stability of these salts at the working temperatures. From (NH₄)₂Mo₆Br₁₄, we could not obtain a single-phase nitride and only a mixture of MoN (JCPDS file 00-025-1367) and Mo₂N (JCPDS file 00-025-1366) can be synthesized (results not shown here). TMB ammonolyses gives the most remarkable results. Two different molybdenum nitrides phases could be obtained at relatively low temperatures: Mo₂N (fcc, $Fm\bar{3}m$) at 450°C and the less-known Mo₅N₆ phase (hcp, $P6_3/m$; JCPDS file 00-051-1326) starting from 500°C. TMB structure consists of molybdenum atoms octahedra with 14 bromine ligands in both apical and inner positions (**Figure 1**). The cluster units are stabilized by (TBA)⁺ counter-cations. TMB crystallizes according to the $P2_1/n$ space group rules¹. The selectivity of TMB, coupled with the fact that molybdenum nitrides are obtained at low

Table 2: Syntheses conditions, crystallites size, elemental analyses and BET specific surfaces areas of Mo₂N and Mo₅N₆ synthesized starting from TMB, MoS₂ and MoO₃. Values given with an uncertainty of 0.5 wt.% for elemental analyses, and 2 m²/g for BET specific surface areas.

	Precursor	Ammonolysis T (°C)	Products	Crystallites size (nm)	N (wt.%)	O (wt.%)	S _{BET} (m ² /g)
TMB-450	(TBA) ₂ Mo ₆ Br ₁₄	450	Mo ₂ N	3	13.2	5.2	80
Mo ₂ N-ref	MoO ₃	700	Mo ₂ N	9	10.6	3.4	50
TMB-650	(TBA) ₂ Mo ₆ Br ₁₄	650	Mo ₅ N ₆	15	13.5	3.2	40
Mo ₅ N ₆ -ref	MoS ₂	690	Mo ₅ N ₆	20	14.6	3.7	30

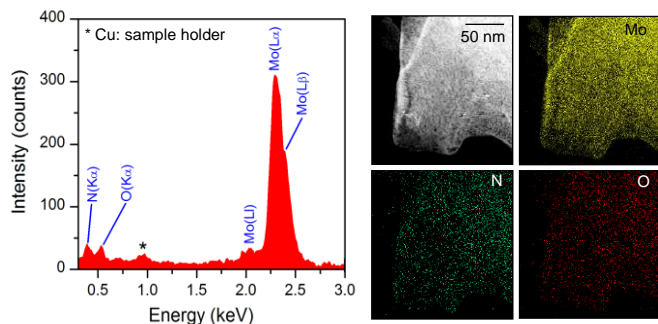


Figure 3. EDS-TEM spectrum of TMB-650 and mapping for molybdenum, nitrogen and oxygen.

temperatures under an ammonia flow in comparison with classic synthetic routes^{3,4} make it a very attractive precursor.

Characterization The original cluster compound TMB is used to synthesize Mo_2N (TMB-450) and Mo_5N_6 (TMB-650) at 450 and 650°C. To compare the impact of such a starting material, these two molybdenum nitride phases were also synthesized as Mo_2N -ref and Mo_5N_6 -ref starting from more conventional precursors: MoO_3 for the synthesis of Mo_2N ³, and MoS_2 for that of Mo_5N_6 ⁴. Synthesis conditions, BET specific surface areas, elemental analyses and crystallites size of these four compounds are given in **Table 2**. Powder-XRD patterns show that all samples can be indexed as pure Mo_2N or Mo_5N_6 (**Figure 2**). However, the extinction of the (101) reflection (22.4° 2θ) is observed for TMB-650. As discussed earlier, the structural resolution of this phase is not complete. Simulated XRD patterns of the Mo_5N_6 models of Tessier and Vajenine (presented in **Figure S1**) are calculated using Vesta Software (**Figure S2**). These two models differ only by the position of the molybdenum vacancies, respectively in octahedral or prismatic sites. When the vacancies are placed in octahedral sites (Tessier model), the extinction of the (101) peak is observed on the XRD pattern. It is then possible that the structures of Mo_5N_6 -ref and TMB-650 are not identical and differs the occupation rate of the positions of the molybdenum sites. Rietveld refinements of all four samples are detailed in the supplementary information (**Figure S3** and **Table S2**). When compared to Mo_2N , TMB-450 shows a shift of the diffraction peaks toward small angles, indicating larger cell parameters. The refined parameter is equal to 4.2147(9) Å for TMB-450 and 4.1609(2) for Mo_2N -ref. The difference between these values and the shift to lower 2 -theta can be explained by the presence of impurities or a molybdenum deficiency, due to low temperature synthesis.

First, Mo_5N_6 samples synthesized starting from TMB were formed at 500°C under ammonia (TMB-500), leading to a higher specific surface area ($50 \text{ m}^2/\text{g}$) than TMB-650, but also to the presence of NH_4Br impurities. Indeed, the reaction between the cluster compound and NH_3 leads to the formation of NH_4Br as a byproduct. NH_4Br is then adsorbed on the nitrides, modifying the basicity of the surface, and reacting with OH_x and CO_2 gas species in

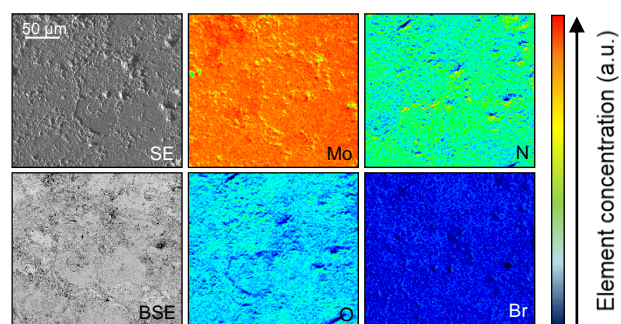


Figure 4. WDS-EPMA mapping for molybdenum, nitrogen, oxygen and bromine on TMB-650.

order to degrade Mo_5N_6 over the time (**Figures S4-S7**). To prevent this phenomenon, the ammonolysis temperature was increased to 650°C, well above the sublimation temperature of NH_4Br (452°C). EDS (coupled with TEM) (**Figure 3**) and WDS-EPMA (**Figure 4**) are used on TMB-650 to check the absence of bromine impurities and observe the repartition of molybdenum and oxygen all over the sample at different scales. EDS spectrum confirms the presence of nitrogen, molybdenum and oxygen. Bromine is not detected on TMB-650 (bromine $L\alpha$ and $L\beta$ edge energies are respectively 1.48 keV and 1.53 keV), proving that increasing the ammonolysis temperature to 650°C is sufficient to avoid the presence of adsorbed NH_4Br on the molybdenum nitrides (**Figure 3**). WDS-EPMA mapping data show a regular distribution of molybdenum and nitrogen all over the sample, proving the homogeneity of TMB-650 (**Figure 4**). As seen by EDS-TEM at a nanoscale, bromine is not detected by this microscale method as well. Ageing studies of TMB-500 and TMB-650 is conducted. Both samples were kept under ambient conditions for 3 months and XRD patterns were recorded every month. TMB-500 is degraded into MoO_2 and MoO_3 after one month, while TMB-650 is perfectly stable after three months (**Figure S7**). Crystallites sizes are extracted from the Rietveld refinements of the XRD patterns (**Table 2** and **Table S2**). Molybdenum nitrides formed from the cluster precursor

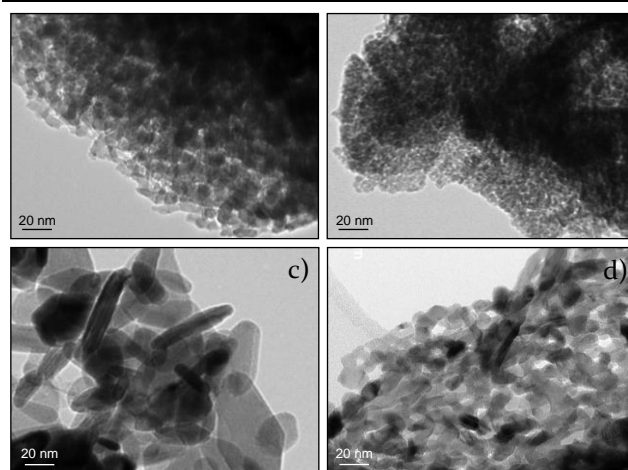


Figure 5. TEM images of Mo_2N -ref (a), TMB-450 (b), Mo_5N_6 -ref (c) and TMB-650 (d).

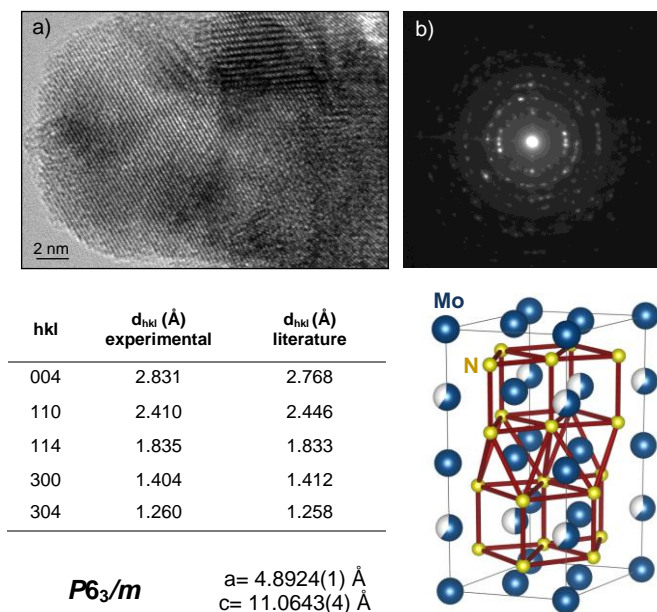


Figure 6. HRTEM image (a), selected area electron diffraction (SAED) pattern image (b) and extracted data from selected area electron diffraction pattern (table) for TMB-650.

contain crystallites with smaller size for both phases compared to reference samples, demonstrating the impact of this new synthetic route. Considering Mo_5N_6 as an example, the size of crystallites is 20 nm using MoS_2 as a precursor versus 15 nm starting from TMB. Specific surface areas are slightly higher following the cluster synthetic route for both Mo_2N and Mo_5N_6 and reach $80 \text{ m}^2/\text{g}$ for TMB-450 proving the role of the nanostructured precursor on the morphology of the resulting nitrides (Table 2). The nitrogen content is higher than the calculated value (6.8 wt.%) for TMB-450 and Mo_2N -ref. This can be explained for both samples by the high surface areas and relatively low synthesis temperatures, leading to adsorption of NH_x species on their surfaces. In addition, TMB-450 contains NH_4Br impurities, contributing to the high nitrogen content. At higher synthesis temperature, adsorption of NH_x species can be avoided: Mo_5N_6 -ref has a nitrogen content close to the calculated value (14.9 wt.%) whereas TMB-650 exhibits a small nitrogen deficiency (13.5 wt.%). Synthesis conditions and precursors preparations are adjusted to limit the presence of oxygen in the nitrides. Indeed, both as-prepared TMB and MoS_2 precursors contain around 4 wt.% of oxygen. It is therefore not straightforward to obtain nitride materials with low oxygen content and high specific surface area. For TMB-650 and Mo_5N_6 -ref, 3.2 to 3.7 wt.% of oxygen are measured. FTIR conducted on TMB-650 (Figure S6) shows peaks characteristic of O-H (1690 cm^{-1}) and H-O-H (3400 cm^{-1}) bonding, indicating that oxygen may be present only under the form of adsorbed water. In addition, ATG-MS analyses are realized on Mo_5N_6 -ref and TMB-650 (Figure S8). We observe a mass loss of 3.9 wt.% and 2.8 wt.% for Mo_5N_6 -ref and TMB-650 up to 500°C , corresponding to OH and

H_2O signals according to MS analysis. This result is in good adequation with the oxygen contents determined by elemental analyses. Thus, it is clear that the oxygen present in the nitride materials is mainly due to adsorbed water on the surface. TEM is first used to observe the shape and size of the particles for the four different molybdenum nitrides samples. TMB-450 and Mo_2N -ref exhibit a similar morphology with round shaped particles of around 15 nm in diameter for Mo_2N -ref and 10 nm for TMB-450. Mo_5N_6 samples consist of platelets aggregates with broad size distribution dimensions. The average length is 60 nm for Mo_5N_6 -ref and 20 nm for TMB-650. This new synthetic route leads to smaller particle sizes. TEM confirms the clear impact of the nanoscaled precursor on the morphology. HRTEM and selected area electron diffraction (SAED) were performed on TMB-650 to verify the crystallinity of this sample and to confirm the data obtained by powder-XRD (Figure 2). Single phase well-crystallized particles are observed by HRTEM for TMB-650 (Figure 6.a.). SAED pattern consists of wide diffraction circles, characteristics of nanocrystals (Figure 6.b.). Experimental d_{hkl} values were extracted from the SAED pattern and compared with those obtained by Tessier et al.⁵ and Vajenine et al.². Good agreement is obtained between our experimental data and the literature values, confirming the powder-XRD results and the presence of pure Mo_5N_6 by ammonolysis of the original TMB precursor. Unfortunately, it was not possible to conclude yet about the uncertainty concerning the ordering of the molybdenum vacancies in Mo_5N_6 either in prismatic or octahedral sites.

Catalytic performance Molybdenum nitrides are tested as heterogeneous catalysts for the WGS. Concerning the light-off tests (5 mol.% CO, 25 mol.% H_2O – flow rate of $80 \text{ mL}/\text{min}$), the results are given in function of the CO percentage conversion (Figure 7) and the normalized rate of the reaction in function of the weight of Mo_5N_6 (Figure S9). TMB-650 shows the highest CO conversion, up to 77 % at 450°C , whereas TMB-450 reaches a CO conversion of only 11 % at the same temperature. It is important to notice that TMB-650 and Mo_5N_6 -ref are the two samples with the most attractive results, giving a potential application for this less explored

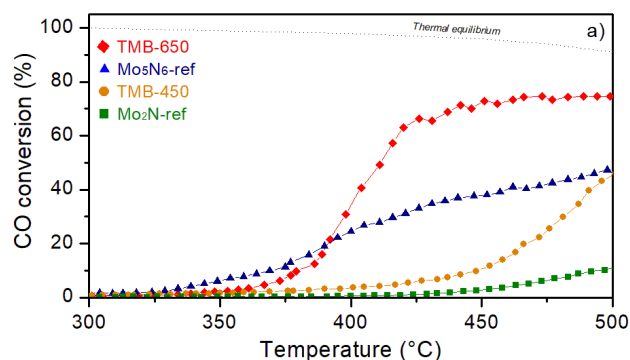


Figure 7. Catalytic performance of the catalysts for the WGS. Light-off curves of TMB-650, Mo_5N_6 -ref, TMB-450 and Mo_2N -ref.

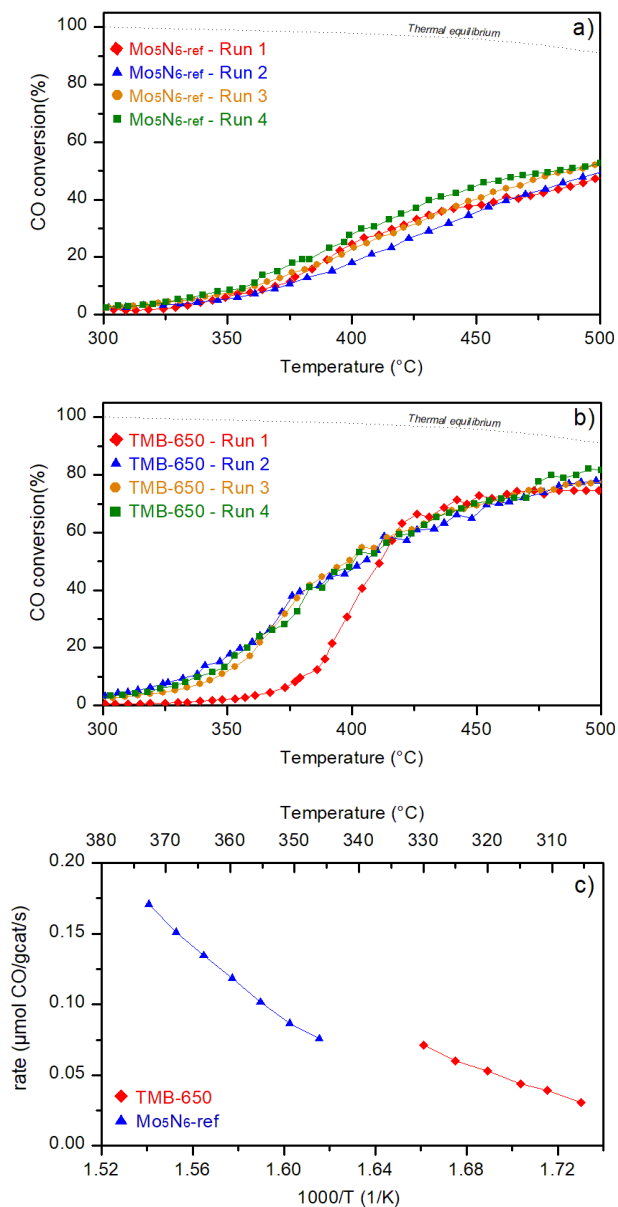


Figure 8. Catalytic performance of the catalysts for the WGSR. Successive light-off curves of Mo₅N₆-ref (a) and TMB-650 (b). Arrhenius plot of the reaction rate after four successive light-off curves (c).

phase. In addition, the two molybdenum nitrides synthesized from the cluster compound precursor TMB-450 and TMB-650 give higher conversions than their counterparts synthesized with more common starting materials. Given the high oxygen content of the as-synthesized molybdenum nitrides, the reactivity of the material under CO only is studied on TMB-650 and presented in **Figure S10**. A single peak is visible, starting at 407 °C for 3 % CO conversion, that is 50 °C higher than under WGSR conditions. The conversion of CO in the absence of H₂O is probably related to the reaction with surface oxygen and partial reduction of Mo₅N₆. The product profile of the test under CO only is presented in **Figure S11**, showing that all the CO is transformed into CO₂ and no byproduct is present. As the WGSR is an endothermic reaction (**Figure 7**: thermal equilibrium)

and the feed contains an excess of water vapor, secondary reaction such as methanation reaction could occur. We do not observe the formation of CH₄, and the carbon balance demonstrates that only CO and CO₂ are present, without the formation of any byproduct (**Figure S12**). Next to the catalytic performance, the stability under tests conditions is one of the most important parameters defining a catalyst material. To investigate the stability of these molybdenum nitrides under WGSR conditions, four successive light-offs are realized on the Mo₅N₆ samples (**Figure 8a and 8b**). The experimental conditions are identical as **Figure 7.a** (5 mol.% CO, 25 mol.% H₂O-flow 80 mL/min). Surprisingly, the catalytic performance of TMB-650 is enhanced for runs 2, 3 and 4, as the CO to CO₂ conversion starts at lower temperature than during the first run. Concerning Mo₅N₆-ref, the four runs lead to identical light-off curves. **Figure 8.c.** shows Arrhenius-type graphs of the steady-state reaction rates, obtained from the fourth run of TMB-650 and Mo₅N₆-ref at low CO conversion (below 15%). The difference between the two catalysts differing only by the precursor is striking, even though the overall performance is lower than any supported noble metal or transition metal catalyst^{41,42}. At the end of the fourth light-off, a dwell of 5 hours at 525°C is performed to look at the stability of the catalysts at high temperature. Both samples are stable for at least 5 hours at 525°C after four successive light-off curves, with a constant CO conversion of 75 % for TMB-650 and a CO conversion of 53 % for Mo₅N₆-ref under our experimental conditions (**Figure 9**).

To study the stability of Mo₅N₆ under reactive conditions, post-catalytic characterizations are carried out, starting with XRD after the third run on both TMB-650 and Mo₅N₆-ref (**Figure 10**). Partial oxidation of both Mo₅N₆ samples is visible in the XRD patterns, characterized by the presence of the (011) and (222) reflections of monoclinic MoO₂. Rietveld refinement shows that the presence of MoO₂ does modify the cell parameters (**Figure S13** and **Table S3**), possibly indicating the presence of Mo-vacancies, as MoO₂ is formed at the same time. Also, the crystallite size is slightly reduced after the catalytic tests. The specific surface area measured on spent TMB-650 and spent Mo₅N₆-ref is 30 and 25 m²/g (compared to 40 and 30 m²/g before catalytic

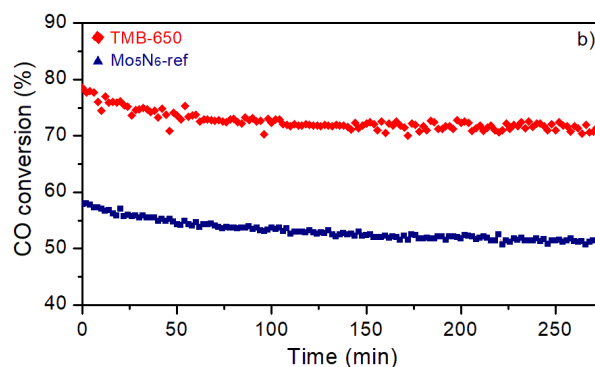


Figure 9. Stability tests (5h at 525°C) for TMB-650 and Mo₅N₆-ref after four consecutive light-off curves.

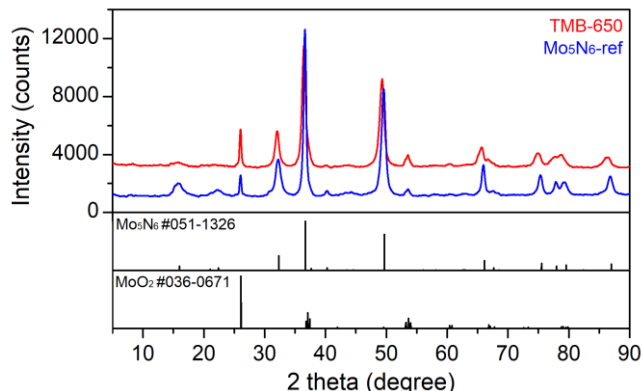


Figure 10. Post-catalysis XRD patterns for Mo_5N_6 -ref and TMB-650 after three WGSR light-off.

tests), indicating a small decrease in the specific surface area. Rietveld analysis further shows that a higher fraction of MoO_2 is present in spent TMB-650 (approx. 15 wt.%) compared to spent Mo_5N_6 -ref (approx. 6 wt.%) after three WGSR light-off. These results are in agreement with results from elemental analyses (Table 3): 8.6 wt.% (O) and 9.6 wt.% (N) for TMB-650 and 6.0 wt.% (O) and 12.2 wt.% (N) for Mo_5N_6 -ref. The larger fraction of MoO_2 and higher oxygen content in TMB-650 might be related to the larger specific surface area. Concerning TMB-650, further elemental analyses are realized between each light-off (Table 3). Partial oxidation of Mo_5N_6 into MoO_2 occurs only during the first light-off, the weight percentages of oxygen and nitrogen are stable after runs 2 and 3. According to these results, surface oxidation occurs on both Mo_5N_6 samples during the first light-off due to the presence of adsorbed water. This is further confirmed when exposing the catalyst to pure water vapor, in the absence of CO and under the same temperature conditions than the catalytic tests. Also, in this case a small fraction (approx. 13 wt.%) of Mo_5N_6 is transformed into MoO_2 , but the main phase is Mo_5N_6 (Figure S14 and Table S4). Even though MoO_2 alone is not highly active for this reaction (Figure S15), TMB-650 shows improved performance upon cycling. Besides the oxidation of Mo_5N_6 into MoO_2 , amorphous surface oxynitrides might have been formed. Liu et al. investigated the role of

Table 3. Elemental analyses on TMB-650 and Mo_5N_6 -ref after each successive light-off curve.

	TMB-650		Mo_5N_6 -ref	
	O (wt.%)	N (wt.%)	O (wt.%)	N (wt.%)
As-synthesized	3.2	13.5	3.7	14.6
1 run WGSR	7.5	9.7		
2 run WGSR	8.4	9.6		
3 run WGSR	8.6	9.6	6.0	12.2

oxygen on the catalytic properties of molybdenum carbides and concluded that the high activity of Mo_2C is due to the presence of an oxycarbide phase in the surface during the WGSR⁴³. The structure difference observed by XRD between TMB-650 and Mo_5N_6 -ref could also explain the enhanced catalytic properties of TMB-650, as this sample may be more lacunar at its surface. Further studies are needed to fully determine the active phase, which goes beyond the scope of this paper.

• CONCLUSION

Nanostructured molybdenum nitrides are synthesized starting from an original precursor: the cluster compound $(\text{TBA})_2\text{Mo}_6\text{Br}_{14}$. Mo_2N and Mo_5N_6 are obtained by ammonolysis of this starting material at relatively low temperatures (450 and 650°C, respectively) in comparison to more common precursors. High surface areas are obtained, making these compounds attractive for applications in heterogeneous catalysis. TEM demonstrates the impact of this kind of precursor on the particle size of the resultant nitride materials. Purity of the products is confirmed by elemental analyses, WDS-EPMA and EDS. All samples were tested for the WGSR. Nitrides synthesized from $(\text{TBA})_2\text{Mo}_6\text{Br}_{14}$ show higher CO conversion than the corresponding reference nitrides. Mo_5N_6 stands out with a 77 % CO conversion at 450°C and a good stability during five hours under test conditions. It is relevant to notice that Mo_5N_6 is a less known phase with only few applications reported yet in the literature^{6,31}. Molybdenum nitrides formed by this innovative synthesis route leads to drastically enhanced catalytic properties for the WGSR. In comparison with the state of the art, Mo_5N_6 does not reach yet the performances of other reported cost-effective catalysts^{44,45}. Impregnation on oxide catalytic support such as CeO_2 ^{45,46} could further enhance the catalytic properties. This work demonstrates that Mo_5N_6 can be an interesting and cost-effective catalyst for the WGS reaction. Moreover, transition metal clusters can be described as a new family of nitrides precursors and can be used to synthesize a large range of nanostructured transition metal nitrides, for various applications in heterogeneous catalysis or photocatalysis.

• ASSOCIATED CONTENT

The supporting information is available at...

Additional information on the different structures of Mo_5N_6 reported in the literature. Details of Rietveld refinements. EDS-TEM spectra and mapping. WDS-EPMA mapping of TMB-450 and TMB-500. FTIR spectra of Mo_5N_6 samples. XRD ageing study of TMB-500 and TMB-650. ATG-MS of TMB-650 and Mo_5N_6 -ref. Rietveld refinement of TMB-650 and Mo_5N_6 -ref after catalytic and hydrothermal tests. Catalytic performance of MoO_2 . Additional SEM images of all samples.

● AUTHOR INFORMATION

Corresponding Authors

*E-mail: kevin.guy@univ-rennes1.fr

*E-mail: franck.tessier@univ-rennes1.fr

*E-mail: helena.kaper@saint-gobain.com

ORCID

Kevin Guy: 0000-0002-2412-0512

Franck Tessier: 0000-0002-1253-7011

Helena Kaper: 0000-0001-8048-9018

Fabien Grasset: 0000-0002-4911-0214

Valérie Demange: 0000-0002-8159-2660

Yoshitaka Matsushita: 0000-0002-4968-8905

Yoshio Matsui: 0000-0002-2044-3450

Tetsuo Uchikoshi: 0000-0003-3847-4781

Naoki Ohashi: 0000-0002-4011-0031

Stéphane Cordier: 0000-0003-0707-3774

Conflicts of interests

All authors have given approval to the final version of the manuscript.

Notes

The authors declare no competing financial interest.

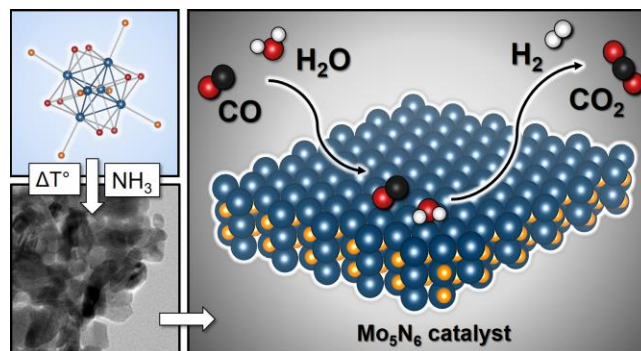
● ACKNOWLEDGMENT

The authors acknowledge the University of Rennes 1 (UR1), Saint-Gobain Research Provence (SGRP), the National Institute for Materials Science (NIMS) and the Centre National de la Recherche Scientifique (CNRS) for the financial support and the access to their different facilities. A part of this work was carried out in the France-Japan international collaboration framework and supported by Kakenhi Grant-in-Aid (No. 19H05818) from the Japan Society for the Promotion of Science (JSPS).

● REFERENCES

- (1) Kirakci, K.; Cordier, S.; Perrin, C. Synthesis and Characterization of $Cs_3Mo_6X_{14}$ ($X = Br$ or I) Hexamolybdenum Cluster Halides: Efficient Mo_6 Cluster Precursors for Solution Chemistry Syntheses. *Z. Für Anorg. Allg. Chem.* **2005**, *631* (2–3), 411–416.
- (2) Ganin, A. Yu.; Kienle, L.; Vajenine, G. V. Synthesis and Characterisation of Hexagonal Molybdenum Nitrides. *J. Solid State Chem.* **2006**, *179* (8), 2339–2348.
- (3) Volpe, L.; Boudart, M. Compounds of Molybdenum and Tungsten with High Specific Surface Area: I. Nitrides. *J. Solid State Chem.* **1985**, *59* (3), 332–347.
- (4) Marchand, R.; Tessier, F.; DiSalvo, F. J. New Routes to Transition Metal Nitrides: And Characterization of New Phases. *J. Mater. Chem.* **1999**, *9* (1), 297–304.
- (5) Tessier, F.; Marchand, R. An Original Way to Prepare Nitride-Type Compounds from Sulfide Precursors. *J. Alloys Compd.* **1997**, *262–263*, 410–415.
- (6) Cao, B.; Neuefeind, J. C.; Adzic, R. R.; Khalifah, P. T. Molybdenum nitrides as oxygen reduction reaction catalysts: structural and electrochemical studies. *Inorg. Chem.* **2015**, *54*, 2128–2136.
- (7) Hargreaves, J. S. J. Heterogeneous Catalysis with Metal Nitrides. *Coord. Chem. Rev.* **2013**, *257* (13), 2015–2031.
- (8) Alexander, A. M.; Hargreaves, J. S. J.; Alternative Catalytic Materials: Carbides, Nitrides, Phosphides and Amorphous Boron Alloys; *Chem. Soc. Rev.* **2010**, *39*, 4388–4401.
- (9) Levy, R. B.; Boudart, M. Platinum-Like Behavior of Tungsten Carbide in Surface Catalysis. *Science* **1973**, *181* (4099), 547–549.
- (10) Blengini, G. A.; Blagoeva, D.; Dewulf, J.; Torres de Matos, C.; Nita, V.; Vidal-Legaz, B.; Latunussa, C. E. L.; Kayam, Y.; Talens Peirò, L.; Baranzelli, C.; Manfredi, S.; Mancini, L.; Nuss, P.; Marmier, A.; Alves-Dias, P.; Pavel, C.; Tzimas, E.; Mathieux, F.; Pennington, D.; Ciupagea, C. *Assessment of the Methodology for Establishing the EU List of Critical Raw Materials*, Publications Office of the European Union, Luxembourg, **2017**, 978-92-79-69612-1.
- (11) Ma, L.; Ting, L. R. L.; Molinari, V.; Giordano, C.; Yeo, B. S. Efficient Hydrogen Evolution Reaction Catalyzed by Molybdenum Carbide and Molybdenum Nitride Nanocatalysts Synthesized via the Urea Glass Route. *J. Mater. Chem. A* **2015**, *3* (16), 8361–8368.
- (12) Morales-Guio, C. G.; Stern, L.-A.; Hu, X. Nanostructured Hydrotreating Catalysts for Electrochemical Hydrogen Evolution. *Chem. Soc. Rev.* **2014**, *43* (18), 6555–6569.
- (13) Chen, W.-F.; Sasaki, K.; Ma, C.; Frenkel, A. I.; Marinkovic, N.; Muckerman, J. T.; Zhu, Y.; Adzic, R. R. Hydrogen-Evolution Catalysts Based on Non-Noble Metal Nickel-Molybdenum Nitride Nanosheets. *Angew. Chem. Int. Ed.* **2012**, *51* (25), 6131–6135.
- (14) Kumar, R.; Rai, R.; Gautam, S.; Sarkar, A. D.; Tiwari, N.; Nath Jha, S.; Bhattacharyya, D.; K. Ganguli, A.; Bagchi, V. Nano-Structured Hybrid Molybdenum Carbides/Nitrides Generated in Situ for HER Applications. *J. Mater. Chem. A* **2017**, *5* (17), 7764–7768.
- (15) Schlatter, J. C.; Oyama, S. T.; Metcalfe III, J. E.; Lambert Jr, J. M. Catalytic Behavior of Selected Transition Metal Carbides, Nitrides, and Borides in the Hydrodenitrogenation of Quinoline. *Ind. Eng. Chem. Res.* **1988**, *27* (9), 1648–1653.
- (16) Katzer, J. R.; Sivasubramanian, R. Process and Catalyst Needs for Hydrodenitrogenation. *Catal. Rev.* **1979**, *20* (2), 155–208.
- (17) Kojima, R.; Aika, K. Molybdenum Nitride and Carbide Catalysts for Ammonia Synthesis. *Appl. Catal. Gen.* **2001**, *219* (1), 141–147.
- (18) Aika, K.; Takano, T.; Murata, S. Preparation and Characterization of Chlorine-Free Ruthenium Catalysts and the Promoter Effect in Ammonia Synthesis: A Magnesia-Supported Ruthenium Catalyst. *J. Catal.* **1992**, *136* (1), 126–140.
- (19) Zeinalipour-Yazdi, C. D.; Hargreaves, J. S. J.; Catlow, C.; R. Nitrogen Activation in a Mars-van Krevelen Mechanism for Ammonia Synthesis on Co_3Mo_3N . *J. Phys. Chem. C.* **2015**, *119* (51), 28369–28376.
- (20) Chen, X.; Zhang, T.; Zheng, M.; Wu, Z.; Wu, W.; Li, C. The Reaction Route and Active Site of Catalytic Decomposition of Hydrazine over Molybdenum Nitride Catalyst. *J. Catal.* **2004**, *224* (2), 473–478.
- (21) Neylon, M. K.; Bej, S. K.; Bennett, C. A.; Thompson, L. T. Ethanol Amination Catalysis over Early Transition Metal Nitrides. *Appl. Catal. Gen.* **2002**, *232* (1), 13–21.
- (22) McGee, R. C. V.; Bej, S. K.; Thompson, L. T. Basic Properties of Molybdenum and Tungsten Nitride Catalysts. *Appl. Catal. Gen.* **2005**, *284* (1), 139–146.
- (23) Bej, S. K.; Thompson, L. T. Acetone Condensation over Molybdenum Nitride and Carbide Catalysts. *Appl. Catal. Gen.* **2004**, *264* (2), 141–150.
- (24) Patt, J.; Moon, D. J.; Phillips, C.; Thompson, L. Molybdenum Carbide Catalysts for Water-Gas Shift. *Catal. Lett.* **2000**, *65* (4), 193–195.

- (25) Dong, J.; Fu, Q.; Jiang, Z.; Mei, B.; Bao, X. Carbide-Supported Au Catalysts for Water–Gas Shift Reactions: A New Territory for the Strong Metal–Support Interaction Effect. *J. Am. Chem. Soc.* **2018**, *140* (42), 13808–13816.
- (26) González, I. D.; Navarro, R. M.; Wen, W.; Marinkovic, N.; Rodríguez, J. A.; Rosa, F.; Fierro, J. L. G. A Comparative Study of the Water Gas Shift Reaction over Platinum Catalysts Supported on CeO₂, TiO₂ and Ce-Modified TiO₂. *Catal. Today* **2010**, *149* (3), 372–379.
- (27) Andreeva, D.; Tabakova, T.; Idakiev, V.; Christov, P.; Giovanoli, R. Au/ α -Fe₂O₃ Catalyst for Water–Gas Shift Reaction Prepared by Deposition–Precipitation. *Appl. Catal. Gen.* **1998**, *169* (1), 9–14.
- (28) Andreeva, D.; Idakiev, V.; Tabakova, T.; Ilieva, L.; Falaras, P.; Bourlinos, A.; Travlos, A. Low-Temperature Water-Gas Shift Reaction over Au/CeO₂ Catalysts. *Catal. Today* **2002**, *72* (1), 51–57.
- (29) Ding, K.; Gulec, A.; Johnson, A. M.; Schweitzer, N. M.; Stucky, G. D.; Marks, L. D.; Stair, P. C. Identification of Active Sites in CO Oxidation and Water-Gas Shift over Supported Pt Catalysts. *Science* **2015**, *350* (6257), 189–192.
- (30) Osman, A. I.; Abu-Dahrieh, J. K.; Cherkasov, N.; Fernandez-Garcia, J.; Walker, D.; Walton, R. I.; Rooney, D. W.; Rebrov, E. A Highly Active and Synergistic Pt/Mo₂C/Al₂O₃ Catalyst for Water-Gas Shift Reaction. *Mol. Catal.* **2018**, *455*, 38–47.
- (31) Jin, H.; Liu, X.; Vasileff A.; Jiao Y.; Zhao Y.; Zheng Y.; Qiao S. Single-Crystal Nitrogen-Rich Two-Dimensional Mo₃N₆ Nanosheets for Efficient and Stable Seawater Splitting. *ACS Nano*. **2018**, *12* (12), 12761–127.
- (32) Kerridge, D. H.; Walker, S. J. Molten Potassium Thiocyanate: The Reactions of Some Compounds of Molybdenum, Rhodium and Silver. *J. Inorg. Nucl. Chem.* **1977**, *39* (9), 1579–1581.
- (33) Tessier, F. Determining the Nitrogen Content in (Oxy)Nitride Materials. *Materials* **2018**, *11* (8), 1331.
- (34) Chein, R. Y.; Yu, C; T. Thermodynamic equilibrium analysis of water-gas shift reaction using syngases-effect of CO₂ and H₂S contents. *Energy* **2017**, *141*, 1004–1018.
- (35) Cotton, F. A. Metal Atom Clusters in Oxide Systems. *Inorg. Chem.* **1964**, *3* (9), 1217–1220.
- (36) Guy, K.; Ehni, P.; Paofai, S.; Forschner, R.; Roiland, C.; Amela-Cortes, M.; Cordier, S.; Laschat, S.; Molard, Y. Lord of The Crowns: A New Precious in the Kingdom of Clustomesogens. *Angew. Chem. Int. Ed.* **2018**, *57* (36), 11692–11696.
- (37) Ehni, P.; Guy, K.; Ebert, M.; Beardsworth, S.; Bader, K.; Forschner, R.; Bühlmeyer, A.; Dumait, N.; Roiland, C.; Molard, Y.; et al. Luminescent Liquid Crystalline Hybrid Materials by Embedding Octahedral Molybdenum Cluster Anions with Soft Organic Shells Derived from Tribenzo[18]Crown-6. *Dalton Trans.* **2018**, *47* (40), 14340–14351.
- (38) Nguyen, N. T. K.; Renaud, A.; Wilmet, M.; Dumait, N.; Paofai, S.; Dierre, B.; Chen, W.; Ohashi, N.; Cordier, S.; Grasset, F.; et al. New Ultra-Violet and near-Infrared Blocking Filters for Energy Saving Applications: Fabrication of Tantalum Metal Atom Cluster-Based Nanocomposite Thin Films by Electrophoretic Deposition. *J. Mater. Chem. C* **2017**, *5* (40), 10477–10484.
- (39) Nguyen, N. T. K.; Renaud, A.; Dierre, B.; Bouteille, B.; Wilmet, M.; Dubernet, M.; Ohashi, N.; Grasset, F.; Uchikoshi, T. Extended Study on Electrophoretic Deposition Process of Inorganic Octahedral Metal Clusters: Advanced Multifunctional Transparent Nanocomposite Thin Films. *Bull. Chem. Soc. Jpn.* **2018**, *91* (12), 1763–1774.
- (40) Costuas, K.; Garreau, A.; Bulou, A.; Fontaine, B.; Cuny, J.; Gautier, R.; Mortier, M.; Molard, Y.; Duvail, J.-L.; Faulques, E. Combined Theoretical and Time-Resolved Photoluminescence Investigations of [Mo₆Br₈Br₆]²⁻ Metal Cluster Units: Evidence of Dual Emission. *Phys. Chem. Chem. Phys.* **2015**, *17* (43), 28574–28585.
- (41) Fu, Q.; Weber, A.; Flytzani-Stephanopoulos, M. Nanostructured Au-CeO₂ catalysts for low-temperature water-gas shift. *Catalysis Letters.* **2001**, *77*, 87–95.
- (42) Li, L.; Song, L.; Wang, H.; Chen, C; She, Y.; Zhan, Y.; Lin, X.; Zheng, Q. Water-gas shift reaction over CuO/CeO₂ catalysts: Effect of CeO₂ supports previously prepared by precipitation with different precipitants. *Int. J. Hydrogen Energy.* **2011**, *36*, 8839–8849.
- (43) Liu, P.; Rodriguez J. A. Water-Gas Shift Reaction on molybdenum carbide surfaces: essential role of the oxycarbide. *J. Phys. Chem. B.* **2006**, *110*, 19418–19425.
- (44) Ratnasamy, C.; Wagner, J. P. Water Gas Shift Catalysis. *Catalysis Reviews* **2009**, *51*, 325–440.
- (45) Ashok, J.; Wai, M. H.; Kawi, S. Nickel-based Catalysts for High-temperature Water Gas Shift Reaction-Methane Suppression *Chem. Cat. Chem.* **2018**, *10*, 3927–3942.
- (46) Djinic, P.; Batista, J.; Pintar, A. Calcination temperature and CuO loading dependence on CuO-CeO₂ catalyst activity for water-gas shift reaction. *Applied Catalysis A* **2008**, *347*, 23–33.



For Table of Content only